CAD System for Liver Diseases using Histological and Imaging features

Gurdeep Singh
M. Tech Scholar, ECE Department, IET,
Bhaddal, Ropar, Panjab

Pradeep Kumar Gaur
Asst. Prof.ECE Department, IET, Bhaddal,
Ropar, Panjab

Abstract

The current work for characterization of liver disease has been carried out using histological and imaging data. The BUPA liver disorders dataset created by University of California, Irvine has been considered as histological data. The ultrasound images of hepatocellular carcinoma (HCC) and Hemangioma (HEM) lesions were taken from ultrasoundcases.info. Laws 'texture features were extracted from these images using Laws' masks of length 3. In CAD system design 1, histological classification of liver diseases has been carried out using SVM classifier. In CAD system design 2, liver disease classification has been carried out using imaging features. Finally in CAD system design 3, liver disease classifications have been carried out using both histological and imaging data features. It is observed that liver disease classification higher accuracy is obtained by combining histological and imaging features.

Keywords: *Histological features, Imaging features, Liver disorders, SVM.*

1. Introduction

Liver is the most vital and largest organ of the human body. It performs many important functions like production and excretion of bile (a digestive fluid), synthesis of cholesterol, production of triglycerides (fats), metabolism of proteins, fats and carbohydrates, storage of vitamins and minerals, synthesis of plasma proteins, breakdown of insulin and other hormones, blood pressure management, blood detoxification, etc. Liver is a metabolically active organ necessary for survival [1].

As liver is the largest solid organ of the human body, it becomes an easy target for many diseases. Liver diseases are widely recognized as an emerging public health crisis particularly in South Asian countries. In clinical diagnosis, liver diseases are always taken seriously as it is a vital organ, which performs very important functions required for sound operation of human body. Liver diseases are classified in two broad categories, i.e., *diffuse liver diseases* and *focal liver diseases [2-14]*.

1.1 Focal Liver Diseases

In focal liver diseases, the abnormality is concentrated in a small localized region of the liver parenchyma which is often referred to as *focal liver lesion* (FLL). Liver Cysts, Hemangioma (HEM, i.e., a primary benign FLL), Hepato-cellular carcinoma (HCC, i.e., a primary malignant FLL) and Metastatic carcinoma (MET, i.e., a secondary malignant FLL), are some of the commonly occurring focal liver diseases [2, 3].

1.2 Hemangioma (HEM)

The HEM is the primary, highly vascular benign FLL which is composed of tiny blood vessels. The sonographic appearance of HEMs varies considerably. In 70 % of cases, HEMs encountered in routine clinical practice are *typical HEMswhich* appear as a round, homogeneous, hyperechoic as well as defined lesion. On the side*Atypical HEMs* can be isoechoic or even hypoechoic. The further details can be found in studies [2-4]. The sample image of HEM is shown in figure1.1.

1.3 Hepatocellular Carcinoma (HCC)

The HCC is also called as malignant hepatoma (liver cancer) or primary malignant FLL.The risk factors which give rise to development of HCC are
(*i*) cirrhosis, (*ii*) chronic infection with the hepatitis B and hepatitis C virus, and (*iii*) metabolic diseases.

The appearance of HCC on B-Mode US depends mostly on whether or not there is underlying cirrhosis. Detecting *small HCCs* (SHCCs) developed on coarse and nodular cirrhotic liver parenchyma presents a daunting challenge for experienced radiologists. On the other hand, the sonographic appearance of a *large HCC* (LHCC) is often

inhomogeneous, whereas SHCCs can be hypoechoic and homogeneous.

Fig 1.1 Hemangioma – Appearnace Homogeniously hyperechoic

The sonographic appearances of SHCC vary from hypoechoic to hyperechoic. The further details can be found in studies [2-4]. The sample image of HCC is shown in figure 1.2.

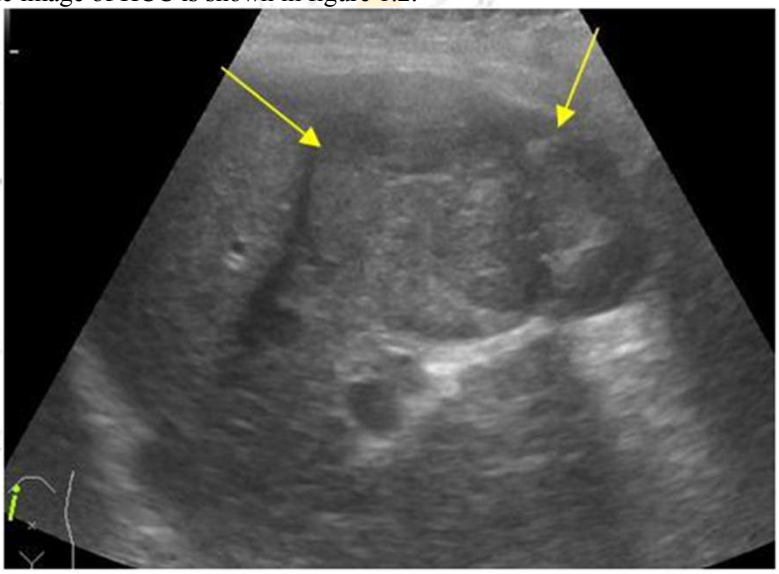

Fig 1.2 HCC ,HCC doesn't bear any typical appearance it can have any sonographic appearance ranging from anechoic to hypo and hyperechoic with homogeneous or heterogeneous texture

The aim of the present research work is to do evaluate the combined diagnostic performance of imaging and histological features for diagnosis of liver diseases. The main objective of the research work is to enhance the diagnostic potential of various forms of diagnosis of liver diseases by developing efficient CAD system designs using a comprehensive and representative histological and image database.

2. Literature Review

Artificial Immune Recognition System (AIRS) classification algorithm, which has an important place among classification algorithms in the field of Artificial Immune Systems, has showed an effective and intriguing performance on the problems it was applied. This framework, named as Fuzzy-AIRS was utilized as a classifier in the conclusion of Liver Disorders, which are of extraordinary significance in prescription. The orders of BUPA Liver Disorders datasets taken from University of California at Irvine (UCI) Machine Learning Repository were finished utilizing 10-overlay cross approval strategy. Achieved grouping correctnesses were assessed by contrasting them and detailed classifiers in UCI site notwithstanding different frameworks that are connected to the related issues. Additionally, the acquired grouping exhibitions were contrasted with AIRS with respect with the arrangement

precision, number of assets and order time. Fluffy AIRS ordered the liver issue dataset with 83.36% precision. Fluffy AIRS acquired the most noteworthy order precision as indicated by the UCI site. Next to of this achievement, Fuzzy-AIRS picked up an essential favorable position over the AIRS by methods for arrangement time. In the trials, it was seen that the arrangement time in Fuzzy-AIRS was diminished around 70% of AIRS. By diminishing order time and additionally acquiring high grouping exactnesses in the connected dataset, Fuzzy-AIRS classifier demonstrated that it could be utilized as a successful classifier for therapeutic issues [2-14].
In the present work an efficient CAD design for liver disorders using histological and imaging data is proposed.

3. Material and Methodology

The experimental flow for designing the proposed CAD system is given in figure3.1.

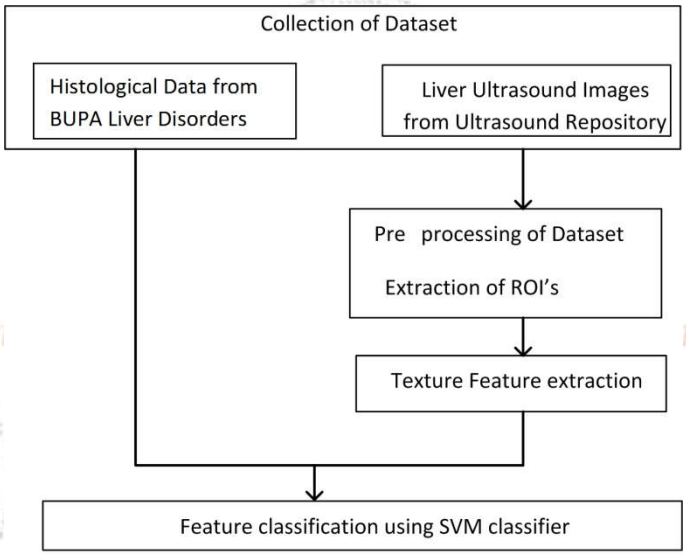

Fig. 3.1 Block diagram of the hybrid CAD system using combined histological & imaging features

3.1 Dataset Description

For experiment 1, the database for liver disorders was taken from University of California, Irvine. This dataset is a standard dataset used globally by researchers working on classification of liver disorders [19]. The description of the dataset is shown in figure 3.2.
The first 5 variables are all blood tests which are thought to be sensitive to Liver disorders that might arise from excessive alcohol consumption. Each line in the BUPA data file constitutes the record of a single male individual.

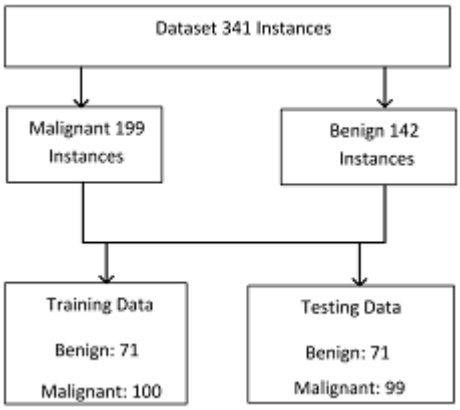

Figure 3.2 Description of BUPA liver disorder datasheet

For experiment 2, the dataset used is the Ultrasound images, which is acquired from [20]. Ultrasound images of Hemangioma and HCC are considered for analysis. The distribution and description of the dataset has been shown in figure 3.3.

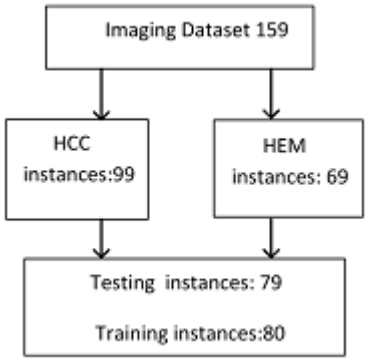

Figure 3.3 Description of datasheet

3.2Feature Extraction

The first CAD system design (experiment 1) uses histological features, which are available in the form of benchmark database available for researchers globally. This database contains the data in form of features in numerical form, which can directly be used for classification. Thus, this system does not require any sort of feature extraction module. The information contained in the database has been explained in table 3.1.

Table 3.1 Attribute information of histological features from BUPA UCI database for Liver disorders

Sr.	Attribute	Information
1	Mean Corpuscular Volume	A measure of the average volume of red blood cells. Normal values: MCV: 80 to 95 femtolitres.
2	Alkaline Phosphotase	An enzyme found in bloodstream. ALP helps break down proteins in the body and exists in different form.
3	Alamine Amino Transferase	The most commonly used indicators of liver damage enzymes normally found in liver cells. Normal Range: Female < 34 IU/L, Male< 45 IU/L
4	AspartateAmino Transferase	Normally found in red blood cells, liver, heart, muscle tissue, pancreas, and kidneys. Normal Range: Female 6 - 34 IU/L,Male 8 - 40 IU/L
5	Gamma-Glutamyl Transpeptidase	Primarily present in kidney, liver, and pancreatic cells. GGT activity is elevated in any and all forms of liver disease. Normal range 7- 35 u/l
6	Drinks	Number of half-pint equivalents of alcoholic beverages drunk per day
7	Selector Field	Used to split data into two sets

The second CAD system design (experiment 2) uses imaging features. The Laws' Masks were then applied to extract the features necessary for classification.

These ROIs were subject to various filters with specific masks to extract the three required fields- Level (L), Edge (E), Spot (S), Ripple (R) and Wave (W).

These masks are created by pre-defined 1-dimensional kernel vectors. In the current work, the masks of

resolution three, five, seven and nine were used [4, 21-24].The different vectors used in Laws' Mask analysis are shown in table 3.2 [24].

Table 3.2 Description of Laws' masks of different lengths

Length of 1-D filter	1-D filter coefficients	No. of 2D Laws' masks	No. of TR images
3	L3=[1, 2, 1] E3=[-1, 0, 1] S3=[-1, 2, -1]	9	6
5	L5= [1, 4, 6, 4, 1] E5= [-1, -2, 0, 2, 1] S5= [-1, 0, 2, 0, -1] W5= [-1, 2, 0, -2 1] R5= [1, -4, 6, -4, 1]	25	15
7	L7= [1, 6, 15, 20, 15, 6, 1] E7= [-1 -4, -5, 0, 5, 4, 1] S7= [-1, -2, 1, 4, 1, -2, -1]	9	6
9	L9= [1, 8, 28, 56, 70, 56, 28, 8, 1] E9= [1, 4, 4, -4, -10, -4, 4, 4, 1] S9= [1, 0, -4, 0, 6, 0, -4, 0, 1] W9= [1, -4, 4, -4, -10, 4, 4, -4, 1] R9= [1, -8, 28, -56, 70, -56, 28, -8, 1]	25	15

Note: TR: rotation invariant texture images.

The 2D masks formed using the above vectors are shown in figure 3.3.

L3L3	E3L3	S3L3
L3E3	E3E3	S3E3
L3S3	E3S3	S3S3

(*a*)

L5L5	E5L5	S5L5	W5L5	R5L5
L5E5	E5E5	S5E5	W5E5	R5E5
L5S5	E5S5	S5S5	W5S5	R5S5
L5W5	E5W5	S5W5	W5W5	R5W5
L5R5	E5R5	S5R5	W5R5	R5R5

(*b*)

L7L7	E7L7	S7L7
L7E7	E7E7	S7E7
L7S7	E7S7	S7S7

(*c*)

L9L9	E9L9	S9L9	W9L9	R9L9
L9E9	E9E9	S9E9	W9E9	R9E9
L9S9	E9S9	S9S9	W9S9	R9S9
L9W9	E9W9	S9W9	W9W9	R9W9
L9R9	E9R9	S9R9	W9R9	R9R9

(*d*)

Fig. 3.3 2-D Laws' masks [24].

(*a*) Nine 2D Law's masks derived from mask length 3. (*b*) Twenty five 2 D Law's masks derived from mask length 5. (*c*) Nine 2D Law's masks derived from mask length 7 (*d*) Twenty five 2D Law's masks derived from mask length 9.

As an example Laws' mask of length 3 is used for explanation purposes. The ROIs are convolved with each of the above nine 2D Laws' masks.

For example an ROI of size M × N is convolved with the mask S5S3 to form texture image (TI_{S5S3}).

$$TI_{S5S3} = ROI \otimes S3S3$$

The mask L3L3 has zero mean and is used to form contrast invariant texture images (TIs).

$$Normalize\,(TI_{mask}) = \frac{TI_{mask}}{TI_{L3L3}}$$

The normalized TIs are passed through a 15 × 15 square window to derive 9 texture energy images (TEMs). The TEM filters perform moving average non-linear filtering operation, i.e.

$$TEM_{i,j} = \sum_{u=-7}^{7} \sum_{v=-7}^{7} |Normalize(TI_{i+u,j+v})|$$

Out of 9TEMs 6 rotationally invariant texture energy images (TRs) are obtained by averaging, i.e.

$$TR_{S_2L_2} = \frac{TEM_{S_2L_2} + TEM_{L_2S_2}}{2}$$

From the derived TRs five statistical parameters i.e. mean, standard deviation, skewness, kurtosis and entropy are computed, thus 30 Laws' texture features (6 TRs × 5 statistical parameters) are computed for each ROI. These statistical parameters are defined as:

$$Mean = \frac{\sum_{i=0}^{M} \sum_{j=0}^{N} (TR_{i,j})}{M \times N}$$

$$SD = \sqrt{\frac{\sum_{i=0}^{M} \sum_{j=0}^{N} (TR_{i,j} - Mean)^2}{M \times N}}$$

$$Skewness = \frac{\sum_{i=0}^{M} \sum_{j=0}^{N} (TR_{i,j} - Mean)^3}{M \times N \times SD^3}$$

$$Kurtosis = \frac{\sum_{i=0}^{M} \sum_{j=0}^{N} (TR_{i,j} - Mean)^4}{M \times N \times SD^4} - 3$$

$$Entropy = \frac{\sum_{i=0}^{M} \sum_{j=0}^{N} (TR_{i,j})^2}{M \times N}$$

The third CAD system design (experiment 3) uses both historical as well as imaging features.

3.3 Classification Module

The LibSVM implementation of SVM classifier has been used extensively for design of CAD systems [15]. In addition to performing linear classification, SVMs can efficiently perform a non-linear classification using what is called the kernel trick, implicitly mapping their inputs into high-dimensional feature spaces.

A support vector machine constructs a hyper plane or set of hyper planes in a high- or infinite-dimensional space, which can be used for classification tasks [21-29].

4. Results and Discussion

The list of experiments carried out in the present work has been tabulated in table 4.1.

Table 4.1 List of Experiments	
Experiment 1	To design CAD system for liver disorders using histological features
Experiment 2	To design CAD system for liver disorders using imaging features
Experiment 3	To design Hybrid CAD system for liver disorders using histological and imaging Features

Experiment 1:

The dataset was classified using the Support Vector Machine classifier. The performance obtained by the above mentioned classification technique on the BUPA UCI Liver disorder dataset is mentioned in table 4.2.

Table 4.2 Performance by SVM classifier using histological features

Classifier	Confusion Matrix (CM)			Classification Accuracy (CA) (%)	S_B (%)	S_M (%)
SVM using histological features		B	M	72.94	59.15	82.83
	B	42	29			
	M	17	82			

Note: S_B: Sensitivity of Benign class, S_M: Sensitivity of Malignant class, B: Benign, M: Malignant

The accuracy of 72.94 % is obtained using SVM classifier.

Experiment 2:

The image dataset was classified using the SVM classifier using and the performance obtained is tabulated in the table 4.3.

Table 4.3 Performance of SVM classifier with Laws' 3 features

Classifier	Confusion Matrix (CM)			Classification Accuracy (CA) (%)	S_B (%)	S_M (%)
SVM using Laws' 3 mask		B	M	74.68	93.33	50.00
	B	42	3			
	M	17	217			

Note: S_B: Sensitivity of Benign class, S_M: Sensitivity of Malignant class, B: Benign, M: Malignant

The maximum accuracy obtained was 74.68% in the case of support vector machine using features derived from Laws' mask of length 3.

Experiment 3:

This CAD system design uses the hybrid features that are combination of histological and imaging features. The dataset was classified using the SVM classification technique the results of classification are shown in table 4.4.

Table 4.4 Performance of SVM classifier using histological and imaging features

Classifier	Confusion Matrix (CM)			Classification Accuracy (CA) (%)	S_B (%)	S_M (%)
SVM using histological and imaging features		B	M	79.74	95.55	58.82
	B	43	2			
	M	14	20			

Note: S_B: Sensitivity of Benign class, S_M: Sensitivity of Malignant class, B: Benign, M: Malignant

Also the best efficiency obtained when Histological and Imaging features have been combined is 79.74 % which is superior in than the classification accuracies obtained using Laws' 3 mask and histological features individually.

5. Conclusion

The current work incorporating the features of both histological and imaging data improved upon the classification efficiency thus making the designed CAD system more efficient and accurate.

REFERENCES

[1] https://en.wikipedia.org/wiki/Liver.

[2] Virmani J, Kumar V, Kalra N and Khandelwal N, "A comparative study of computer-aided classification systems for focal hepatic lesions from B-mode ultrasound, Journal of Medical Engineering and Technology, 2013, vol. 37, pp. 292-306.

[3] Virmani J, Kumar V, Kalra N and Khandelwal N, "Characterization of primary and secondary malignant liver lesions from B-mode ultrasound", Journal of Digital Imaging, 2013, vol. 26, pp. 1058-1070.

[4] Manth N, Virmani J, Kumar V, Kalra N and Khandelwal N, "Application of texture features for classification - 1593.

[6] Ultrasound imaging of primary benign and primary malignant focal liver lesions", in Image Feature Detectors and Descriptors, A.I. Awad and M. Hassaballah (eds.), Switzerland, Springer, 2016, vol. 630.

[7] Kumar SS and Devipal D, "Survey on recent CAD system for liver diseases" in Proceedings of International Conference o, pp. 385-409.

[8] Virmani J, Kumar V, Kalra V and Khandelwal N, "Neural network ensemble based CAD system for focal liver lesions from B-mode ultrasound", Journal of Digital Imaging, 2014, vol. 27, pp. 520-537.

[9] Virmani J, Kumar V, Kalra V and Khandelwal N, "Prediction of cirrhosis from liver ultrasound B-mode images based on Laws' mask analysis", in Proceedings of IEEE International Conference on Image Information Processing, ICIIP-2011. Himachal Pradesh, India, 2011, pp. 1-5.

[10] Fukushima M, Ogawa K, Kubota T and Hisa N, "Quantitative tissue characterization of diffused liver diseases from ultrasound images by neural network", in Proceedings of IEEE Nuclear Science Symposium. Albuquerque, USA, 1997, pp. 1233-1236.

[11] Parker KJ, "Ultrasonic attenuation and absorption in liver tissue", Ultrasound in Medicine and Biology, vol. 9, no. 4, pp. 363-369, 1983.

[12] Schlaps D, Räth U, Volk JF, Zuna I, Lorenz A, Lehmann KJ, Lorenz D, Van Kaick G, Lorenz WJ. Ultrasonic tissue characterization using a diagnostic expert system. In Information processing in medical imaging 1996 (pp. 343-363). Springer Netherlands.

[13] Kadah YM, Farag AA, Zurada JM, Badawi AM, Youssef AB. Classification algorithms for quantitative tissue characterization of diffuse liver disease from ultrasound images. IEEE transactions on Medical Imaging. 1996 Aug;15(4):466-78.

[14] Polat K, Şahan S, Kodaz H, Güneş S. Breast cancer and liver disorders classification using artificial immune recognition system (AIRS) with performance evaluation by fuzzy resource allocation mechanism. Expert Systems with Applications. 2007 Jan 31;32(1):172-83.

[15] Chang CC, LIBSVM A library for support vector machines, 2001. Software available at http://www. csie. ntu. edu. tw/cjlin/libsvm. 2012.

[16] Virmani J, Kumar V, Kalra N, Khandelwal N. SVM-based characterization of liver cirrhosis by singular value decomposition of GLCM matrix. International Journal of Artificial Intelligence and Soft Computing. 2013 Jan 1;3(3):276-96.

[17] Hassanien AE, El-Bendary N, Kudělka M, Snášel V. Breast cancer detection and classification using support vector machines and pulse coupled neural network. InProceedings of the Third International Conference on Intelligent Human Computer Interaction (IHCI 2011), Prague, Czech Republic, August, 2011 2013 (pp. 269-279). Springer Berlin Heidelberg.

[18] Amendolia SR, Cossu G, Ganadu ML, Golosio B, Masala GL, Mura GM. A comparative study of k-nearest neighbor, support vector machine and multi-layer perceptron for thalassemia screening. Chemometrics and Intelligent Laboratory Systems. 2003 Nov 28;69(1):13-20.

[19] M. Lichman, UCI Machine Learning Repository [http://archive.ics.uci.edu/ml]. Irvine, CA: University of California, School of Information and Computer Science, 2013.

[20] http://www.ultrasoundcases.info/Case-List.aspx?cat=137.

[21] Laws KI. Rapid texture identification. In24th annual technical symposium 1980 Dec 23 (pp. 376-381). International Society for Optics and Photonics.

[22] Rachidi M, Marchadier A, Gadois C, Lespessailles E, Chappard C, Benhamou CL. Laws' masks descriptors applied to bone texture analysis: an innovative and discriminant tool in osteoporosis. Skeletal radiology. 2008 Jun 1;37(6):541-8.

[23] Virmani J, Dey N, Kumar V. PCA-PNN and PCA-SVM based CAD systems for breast density classification. InApplications of intelligent optimization in biology and medicine 2016 (pp. 159-180). Springer International Publishing.

[24] Kriti, Virmani J. Breast density classification using Laws' mask texture features. International Journal of Biomedical Engineering and Technology. 2015;19(3):279-302.

[25] Kumar, I., Bhadauria, H.S. and Virmani, J. 'Wavelet packet texture descriptors based four-class BIRADS breast tissue density classification', Procedia Computer Science, Vol. 70, 2015, pp.76–84.